Title

Mechanical Design and Analysis of a Unilateral Cervical Spinal Cord Contusion Injury Model in Non-Human Primates

Journal

Journal of Neurotrauma, 33(12)

ISSN

0897-7151

Authors

Sparrey, Carolyn J
Salegio, Ernesto A
Camisa, William
et al.

Publication Date

2016-06-15

DOI

10.1089/neu.2015.3974

Peer reviewed

JOURNAL OF NEUROTRAUMA 33:1136–1149 (June 15, 2016)

DOI: 10.1089/neu.2015.3974

Mechanical Design and Analysis of a Unilateral Cervical Spinal Cord Contusion Injury Model in Non-Human Primates

Carolyn J. Sparrey,[1,2] Ernesto A. Salegio,[3] William Camisa,[4] Horace Tam,[1] Michael S. Beattie,[3] and Jacqueline C. Bresnahan[3]

Abstract

Non-human primate (NHP) models of spinal cord injury better reflect human injury and provide a better foundation to evaluate potential treatments and functional outcomes. We combined finite element (FE) and surrogate models with impact data derived from *in vivo* experiments to define the impact mechanics needed to generate a moderate severity unilateral cervical contusion injury in NHPs (*Macaca mulatta)*. Three independent variables (impactor displacement, alignment, and pre-load) were examined to determine their effects on tissue level stresses and strains. Mechanical measures of peak force, peak displacement, peak energy, and tissue stiffness were analyzed as potential determinants of injury severity. Data generated from FE simulations predicted a lateral shift of the spinal cord at high levels of compression (>64%) during impact. Submillimeter changes in mediolateral impactor position over the midline increased peak impact forces (>50%). Surrogate cords established a 0.5 N pre-load protocol for positioning the impactor tip onto the dural surface to define a consistent dorsoventral baseline position before impact, which corresponded with cerebrospinal fluid displacement and entrapment of the spinal cord against the vertebral canal. Based on our simulations, impactor alignment and pre-load were strong contributors to the variable mechanical and functional outcomes observed in *in vivo* experiments. Peak displacement of 4 mm after a 0.5N pre-load aligned 0.5–1.0 mm over the midline should result in a moderate severity injury; however, the observed peak force and calculated peak energy and tissue stiffness are required to properly characterize the severity and variability of *in vivo* NHP contusion injuries.

Key words: finite element; primate; simulation; stiffness; strains

Introduction

Impact mechanics and the consequent neural injury are the most significant predictors of long-term neurological function after spinal cord injury (SCI).[1,2] The contusion model, first described by Allen[3] more than 100 years ago, is thought to provide one of the best representations of human injury,[4] although other injury mechanisms are also being studied.[5–8]

Contusion models have been predominantly standardized in rodents, have advanced our understanding of the injury process, and have provided a mechanism for pre-clinical study of therapeutic strategies. Therapies that have demonstrated success in rodent pre-clinical models, however, have yet to be translated into effective clinical treatments.[9] This lack of translation may be, in part, because of differences between rodents and humans, a translational barrier identified by experts in the field; hence, the urgency to characterize a more ''human-like'' animal model in non-human primates (NHP).[10,11]

Recent anatomical evidence in NHPs highlights a previously unknown, spontaneous regeneration of the corticospinal tract after a spinal cord hemisection,[12] a critical observation that appears to be species-specific. In addition, advanced forelimb and hindlimb dexterity in NHPs allows for a more detailed assessment of functional recovery, particularly during fine-motor tasks. Higher vertebrate models of SCI better reflect neuroanatomical and behavioral characteristics of human injury/recovery and provide a better foundation to evaluate complex treatments and functional outcomes.[10,13,14]

The use of NHPs, however, is constrained by ethical issues and costs, and so NHP models of SCI have been used only sparingly. Optimization of NHP SCI models is needed to provide the most

[1]Mechatronic Systems Engineering, Simon Fraser University, Surrey, British Columbia, Canada.
[2]International Collaboration on Repair Discoveries (ICORD), Vancouver, British Columbia, Canada.
[3]Department of Neurological Surgery, Brain and Spinal Injury Center, University of California at San Francisco, San Francisco, California.
[4]Taylor Collaboration, St Mary's Medical Center, San Francisco, California.

information using the least number of animals as possible, and this requires the development of a reliable and repeatable NHP injury model in which the mechanical parameters of impact are well controlled and documented.

Development of a standardized animal model of spinal cord contusion injury relies on establishing a consistent and well-characterized relationship between impact parameters and functional outcomes. Mechanical parameters of impact have been well correlated with functional outcomes and tissue damage in rat[15–19] and mouse[20–22] models of contusion injury; however, a large number of animal experiments were required to establish these standard impact parameters. In fact, more than 10% of animals are often removed from studies because of problems with the mechanical impact such as slippage in the clamps[19,23] or acute mortality.[7]

Mechanistically, injury severity has been previously defined by measuring peak force,[24] peak displacement,[25] or peak energy[26] depending on the injury paradigm implemented. Variability within injury groups remains a challenge for *in vivo* models, and this may reduce the ability of animal models to detect drug-related therapeutic effects. In SCI rat models, standardizing animal parameters such as age, anesthesia, and timing of injury[27] and establishing a zero position for displacement-based impacts[25] have been shown to reduce variation in injury outcomes.

Unilateral contusion models have the additional challenge of lateral cord shift during impact.[28] Angled impacts and variations in impactor alignment have been proposed as methods to ensure consistent ipsilateral cord injury without contralateral involvement.[28,29] Experimental data on spinal contusion injuries in NHPs is sparse, and those available used weight drop systems to generate injuries and did not directly investigate the mechanics of cord impact.[30,31] Therefore, the mechanical parameters required to generate a moderate, unilateral cervical SCI in the NHP are unknown.

Finite element (FE) and surrogate models of the spinal cord are valuable tools to study the mechanics of spinal cord impact without the costs and logistical challenges associated with animal studies. Several groups have established validated approaches to simulate spinal cord injury through FE methods[32–36] and physical surrogate models.[37,38] FE models have demonstrated a strong correlation between tissue level stress, strain, and structural damage in rat models of contusion and dislocation[34,35] and guinea pig white matter lesions.[32,33] The relationship between impact mechanics and tissue damage demonstrate that FE models can be valuable in predicting approximate injury severity for different impacts.

Surrogate models of spinal cords provide another means to quantify impact mechanics. Previous surrogate systems have been validated against *in vivo* experiments[38] and have established the importance of the cerebrospinal fluid (CSF) and dura mater in distributing direct impacts on the spinal cord.[36] Surrogate models have also quantified the effects of the amount of CSF and dural thickness on impact mechanics.[37] Results from tests conducted on surrogate cords highlight the sensitivity of impact mechanics to spinal cord and column morphology. Therefore, developing models that accurately replicate the morphology of the NHP will help to identify mechanical parameters needed to generate consistent injuries with similar behavioral and anatomical outcomes.

The primary goals of this study were to integrate FE and surrogate models with mechanical analyses to define an impact protocol and provide insights into the development of a unilateral, cervical contusion injury in *Macaca mulatta,*[39] equivalent to a previously established rat model.[19] The aim was to minimize the number of live animals required to characterize an NHP model of injury by combining FE analysis, surrogate models, and mechanical analysis of *in vivo* impacts.

Our specific objectives were to: (1) estimate the peak displacement of a unilateral, cervical spinal cord impact in NHPs that mimics established rat models of unilateral contusion[20] using FE models, (2) quantify a starting position to initiate the contusion impact (i.e., mediolateral position and dorsoventral/anteroposterior from the dural surface) to ensure repeatable contusion injuries from a similar starting point and reduce lateral shift of the spinal cord, and (3) calculate the stiffness, impact force, and energy of each *in vivo* impact in NHPs, compare these values with the FE and surrogate model predictions, and refine the *in vivo* impact parameters based on the results of the combined analysis.

Methods

Scaling injury mechanics

Three dimensional (3D) FE models of rat and NHP spinal cords were constructed to simulate the response of the cervical spinal cord to unilateral contusion and to determine the impact protocol for NHPs that would generate a unilateral injury with similar magnitudes of functional and histological outcomes to established rat models.[19] Measurements of spinal cord and column cross-sections of rats (male Long Evans rats, $n=5$, 229 ± 4 g and 84 ± 1.5 days) and NHPs (*Macaca mulatta*; $n=7$; adult males) were obtained from magnetic resonance image (MRI) scans acquired at the cervical level for previous studies.[40,41] Measurements were taken at several spinal levels and averaged over C1–C6. The average rat and primate spinal cord cross-sections were then extruded (10 mm in the rat and 20 mm in the primate) to create 3D FE models (Fig. 1) (ABAQUS/explicit version 6.10, Simulia Inc, Providence RI).

The FE models provided an opportunity to study and compare mechanistic differences in the total amount of CSF and extradural space protecting the cervical spinal cord between these two species. The spinal canal was modeled as a rigid body, providing resistance to support the spinal cord during the contusion impact. Although the spinal canal is not precisely rigid during *in vivo* impact, the combined use of a stereotactic frame to fix the spinal posture and spinal clamps on the spinous processes immediately above and below the site of impact stabilize the column and limit bulk spinal motion.

The impactor was also modeled as a rigid body for computational efficiency. The impactor stiffness is several orders of magnitude greater than the tissue stiffness, resulting in negligible deformation in the impactor during these impacts. The spinal cord and CSF were modeled with 8-node linear brick, reduced integration elements with hourglass control.

The dura mater could not be easily identified in the MRI scans and has thickness ranging from 80–300 μm in humans[42,43] and was previously modeled as 200 μm in rats.[44,45] Therefore, dura mater for the rat and NHP models was created by defining a surface around the CSF layer that was 200 μm thick. The dura was modeled with a four-node doubly curved thin shell element with reduced integration, hourglass control, and finite membrane strains. The gray and white matters were modeled together, because individual characteristics for these materials at high strain rates have not been clearly established.[34,35]

Spinal cord elements were tied to CSF elements, and these were then also tied to the dural shell elements to enforce displacement compatibility. The spinal cord was modeled as a cranial/caudal symmetrical structure at the injury epicenter to reduce computational costs. The symmetry condition also limited bulk motion of the spinal cord. Motion at the end of the spinal cord away from the injury epicenter was constrained in all directions to simulate the effect of cord tethering in the spinal canal. Contact between the dura and canal space was modeled as a hard, frictionless contact. Non-linear analysis was used to account for the large deformations in the tissues.

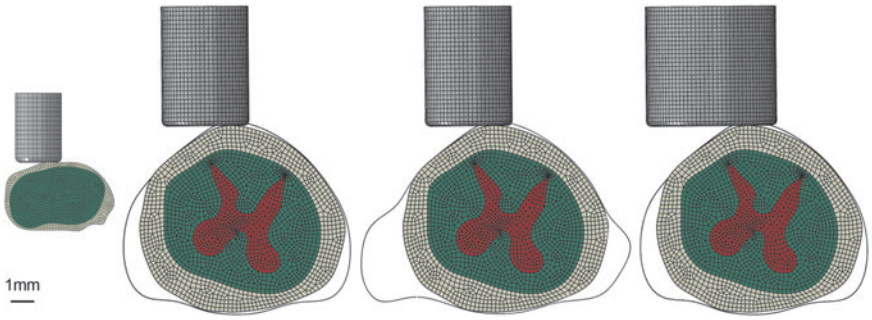

FIG. 1. Material distribution and spinal cord and column morphology in the (from left to right) rat 2 mm impactor, primate 4 mm impactor closed canal, primate 4 mm impactor intervertebral foramen, primate 6 mm impactor. The spinal cord parenchyma (green–white matter, red–gray matter) was modeled as a uniform material. The cerebrospinal fluid space (beige) was bounded by a dural membrane. The cord complex was surrounded by a rigid shell to represent the bounding effect of the boney spinal canal. Color image is available online at www.liebertpub.com/neu

The same material characteristics were assigned to both the rat and primate models, because the limited literature for spinal cord material properties shows consistent properties across several species.[46] Similar to previously developed and validated models of rat SCI, the spinal cord and dura were modeled with Ogden hyperelastic material models and Prony series viscoelastic expansions (Table 1).[34,35] The CSF was modeled as a viscoelastic Mooney-Rivlin material with low shear modulus and moderate bulk modulus.[34,47] This assumption was made based on a brain injury model that showed a viscoelastic material model for CSF did not significantly affect overall brain position calculations compared with a fluid model[47] and greatly reduced computational time.

Spinal cord compression loading was simulated with flat-tipped impactors to match the impactor size and impact depth of established unilateral contusion injury models of rat cervical SCI and scaled to the NHP model using the anterior/posterior (a/p) diameter of the respective spinal cords. The 6 mm impactor was determined by scaling the impactor size from the rat model ($d_{rat} = 2$ mm) using the a/p cord diameter; however, the rat spinal cord has a greater medial/lateral to a/p cord diameter ratio than the primate.

Table 1. Material Property Assignments for the Rat and Primate Unilateral Cervical Spinal Cord Contusion Injury Finite Element Models

Material	*Hyperelastic law*	*Hyperelastic constants*	*Viscoelastic law*	*Viscoelastic constants*
Spinal cord	Ogden	$\mu = 32$kPa $\alpha = 4.7$ $v = 0.45$	Prony	g1 = 0.528 T1 = 0.008 s g2 = 0.3018 T2 = 0.15 s
Dura	Ogden	$\mu = 1205$ kPa $\alpha = 16.2$ $v = 0.45$	Prony	g1 = 0.318 T1 = 0.0009 s g2 = 0.1238 T2 = 0.081 s g3 = 0.0997 T3 = 0.564 s g4 = 0.0997 T4 = 4.69 s
CSF	Mooney-Rivlin	C10 = 125Pa C01 = 125Pa v = 0.49999	Prony	g1 = 0.95 T1 = 0.002 s

CSF, cerebrospinal fluid.

Positioning a 6 mm impactor to avoid contact with the lateral spinal canal to induce a unilateral spinal cord lesion in an NHP model resulted in the medial edge of the impactor crossing the midline and risked affecting the contralateral side of the cord. Therefore, a 4 mm impactor was also evaluated to ensure impact effects could be confined to one side of the cord and thus result in a unilateral lesion.

The impact depth needed to create moderate to severe unilateral cervical contusion injuries in the rat ranged from 1.5 mm–1.8 mm.[28,29] Scaling the contusion depth to the average (a/p) diameter of rat cervical dural sac (2.74 mm), impacts ranged from 55–66% of total dural diameter. Scaling the range of compression to the average primate cervical dural sac a/p diameter (8.55 mm) resulted in equivalent primate impacts of 4.68–5.62 mm.

To fully explore the range of compressive responses in the NHP FE models, peak displacements of 3.8–6.3 mm were simulated. The impact epicenter in the *in vivo* contusion was positioned in the rostral/caudal direction relative to the lamina. Therefore, the location of injury relative to the intervertebral foramen was not clear. The variations in the cord constraint relative to the foramen were assessed using two different spinal cord cross sections (Fig. 1).

Peak forces derived from each impact injury were recorded from the reaction force in the reference node of the impactor. Impact forces in the rat simulations were validated with published experimental results to confirm the accuracy of the current model.[28,29] Maximum principal strains[35] and maximum principal stresses[33] were compared between the rat and NHP models and were used to predict injury patterns in the NHP FE model simulations.

The impact depth and impactor size were selected for the NHP based on the FE model injury pattern predictions at the injury epicenter that best matched the rat contusion models without crossing to the contralateral cord. Bulk motion of the spinal cord in the canal space was also noted.

Defining a baseline for impact

Experimentally, a challenging aspect when attempting to generate a unilateral impact to the cord has been the ability of the cord to shift laterally (i.e., away from the direction of impact). This lateral motion is a result of the eccentric impact between the impactor tip and the spinal cord. The center of mass of the impactor is offset from the center of mass of the spinal cord, which results in the cord having a lateral component of motion as well as rotation. Because of this induced lateral motion and rotation, the large canal space and CSF layer around the primate spinal cord, which provide protection by dissipating the impact across the spinal cord,[36] also enable substantial (2–3 mm) lateral motion in a unilateral impact. To reduce lateral shift in the spinal cord during impact and to minimize the impact dissipation effect of the dura and CSF, the

effect of ''pre-loading'' the spinal cord before impact was explored in the FE and surrogate cord models.

A surrogate spinal cord complex was used to confirm the forces associated with dural surface contact, cord contact, and cord impingement against the canal. The transparent polyethylene tubing used for the surrogate dura mater allowed for visualization of the cord throughout the pre-loading protocol to clearly define the points of contact. The surrogate model of the NHP spinal cord, CSF, and dura was constructed following an approach defined for a surrogate cord model of the human spinal cord.[37] The spinal cord was cast from two part silicone, (QM Skin 30, Quantum Silicones, Richmond, VA) and the dura mater was simulated by polyethylene lay flat tubing that was vacuum sealed at a length of 150 mm and diameter of 12 mm.

The unique features of this surrogate model were: (1) the use of a geometrically accurate primate spinal cord obtained from 3D reconstructions of MRIs acquired from the NHP spinal cord and rapid prototyping a mold for the spinal cord, and (2) sealing of the cord within a saline-filled polyethylene tubing to simulate a pressurized system without the complications of reservoirs and water columns. The surrogate spinal cord complex was supported in a Styrofoam block with a semicylindrical metal trough (6 inch stainless steel scoopula) embedded to simulate the boundary condition of the spinal canal (Fig. 2).

A Bose Electroforce Actuator system (Model 200N LM1, Bose Corporation) was used to apply the pre-loading protocol to the surrogate cord complex (Fig. 2). Details of the impact system are outlined in the companion article[39]; briefly, the impactor system consists of an electromagnetic actuator capable of high precision motion (0.001 mm) at high rates (up to 1 m/sec) and records forces with a precision load cell (100 N). The impactor tip can be positioned to submillimeter accuracy (0.01 mm) in 3D space using manual linear bearing slides mounted with caliper scales. For surrogate cord testing, the system was mounted in a fixed collar attached to a test table. The same mounting collar was used to attach the system to the stereotactic frame for *in vivo* impacts using a press fit with a securing pin for extra support.

To establish a baseline for impacts, slow mechanical indentations on the surrogate dural surface were used to define a ''touch'' protocol that was indicative of the impactor tip making contact with the dorsal aspect of the dura. The surrogate spinal cord was then pre-loaded by slowly advancing the impactor to temporarily displace the CSF, essentially trapping the spinal cord against the bottom of the vertebral canal before impact. The peak pre-load force that corresponded to the trapped spinal cord was recorded to define the spatiotemporal baseline for the unilateral contusion injury.

Post-impact analysis and iterative model refinement

To identify variations in *in vivo* impact parameters, mechanical data from the primate impacts[39] were analyzed to determine the stiffness of the spinal cord. Energy of impact was calculated as the area under the stiffness (force/deformation) curve for each injury. Force traces generated from surrogate and FE tests and the stiffness behavior were compared to the *in vivo* results to determine the accuracy of the models.

In any impact or indentation protocol, the force reading from the load cell attached to the impactor tip is affected by the inertia of the mass of the impactor suspended under the load cell. Although the mass of the impactor is small, the acceleration can be high, and thus the inertial effects cannot be ignored. Inertia compensation is therefore required to determine the actual force applied to the spinal cord during injury. A combination of mass correction and air hit subtraction were used to determine the net force acting on the spinal cord during impact.

To ensure the initial impacts did not create severe injuries, the first two *in vivo* NHP impacts were conducted to generate mild injuries pre-load forces of 0.3 N (approximately 3 mm displacement) with peak impact displacement of 2 mm from the pre-load position (total 5 mm compression). These impacts, however, resulted in no noticeable functional deficits or histological damage[39] and low impact forces. In addition, concerns were raised about the lateral shift of the cord observed even with pre-load contact.

Further FE modeling and surrogate testing were conducted to determine the effect of impactor alignment on injury predictions. The position of the impactor tip was varied from having the medial edge of the impactor aligned with the cord midline to 0.5 mm and 1.0 mm to the contralateral side to refine the impact protocol for subsequent *in vivo* impacts.

Results

General impact characteristics

The FE method was validated by comparing the unilateral impact results from the rat simulations using a 1.6 mm diameter impactor tip

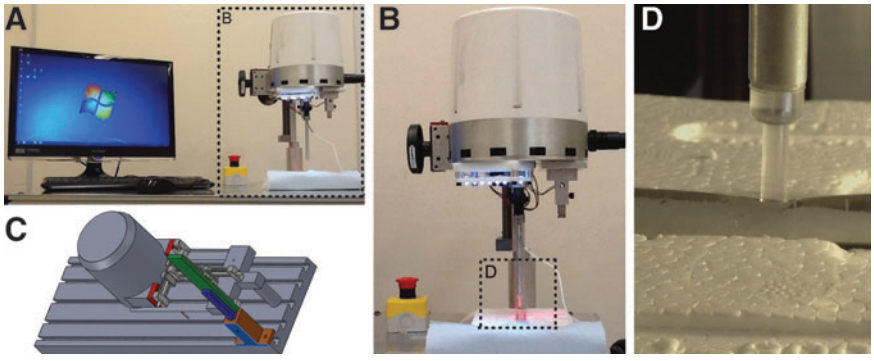

FIG. 2. The surrogate cord model undergoing unilateral contusion with the same impactor as the one used to generate *in vivo* primate contusion injuries. The impact system could be set up on a test cart (**A**) or the surgical table. The impact system was driven by a Bose electromagnetic actuator (**B**) and could be positioned in three-dimensional space using screw-driven, linear bearing slides. The impactor could be move from the test table to attach to the stereotaxic frame using a single mounting post (**C**). To calibrate the impact mechanics, tune the controls of the Bose actuator and verify the behavior of the system before each surgery; the impact protocol was run using a surrogate spinal cord complex (**D**). The surrogate spinal cord is visible through the transparent dura (i.e., polyethylene lay flat tubing), making it possible to visualize contact between the dural surface and the cord. Note the local displacement of saline (i.e., cerebrospinal fluid) under the impactor's tip due to pre-loading. Color image is available online at www.liebertpub.com/neu

with published experimental results using the same sized impactor tip. Peak forces (2.88 ± 0.10 N) at fixed displacements (1.6–1.8 mm) in the FE model with the impactor aligned with the midline were slightly higher than experimental results for moderate unilateral contusion injuries from a force controlled system that reported peak forces of 200 kdyn (2 N) for impact displacements of 1.6–1.8 mm when the impactor was positioned midway between the median dorsal vein and the lateral edge of the spinal cord.[29]

The FE analysis demonstrated similar peak strains (Fig. 3) and stresses (Fig. 4) for mild/moderate impacts (<56% compression) when impact was initiated from the dural surface despite the thicker CSF layer and angled canal geometry in the NHP spinal canal.

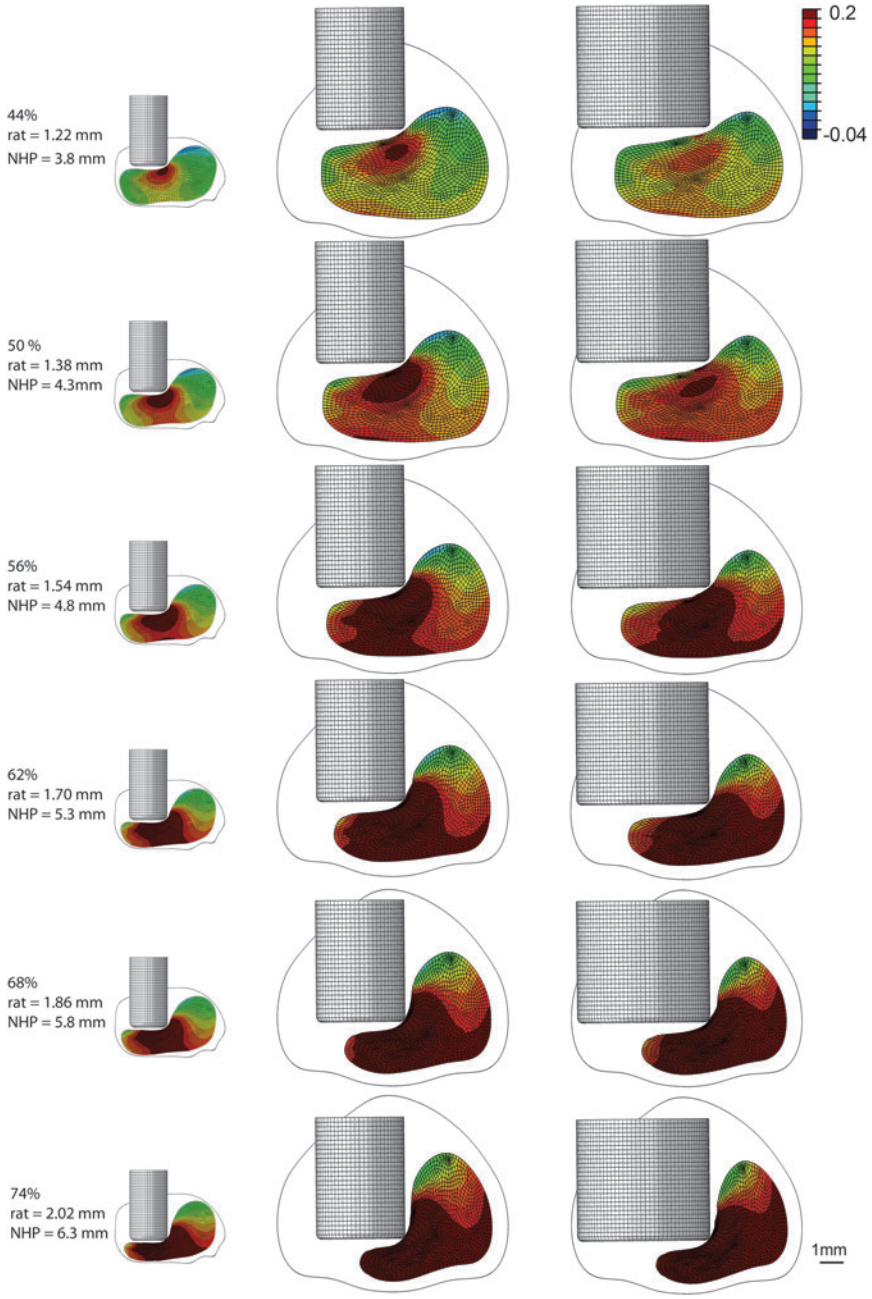

FIG. 3. Maximum principal strains in the spinal cord resulting from unilateral contusion injuries in the rat (left) and primate (middle = 4 mm impactor, positioned 0.5 mm over midline, right = 6 mm impactor, positioned 0.5 mm over midline). The impactor is contacting the dorsal surface of the dura in each model. Impactor peak displacement, measured from the undeformed dural surface, increases from 44% to 74% of the dural sac anterior/posterior diameter from the top to bottom rows, respectively. The corresponding magnitude of compression is listed for the rat and non-human primate (NHP) models. Peak strains above 20% were mostly confined to the ipsilateral spinal cord in NHP models with a 4 mm impactor up to impact depths of 4.8 mm, but spread to the contralateral cord in all 6 mm impacts and with compression greater than 4.8 mm in the 4 mm impacts. All impacts, except the most severe NHP models, showed an area of lower strains in the peripheral white matter of the ipsilateral spinal cord. Geometry of the vertebral canal is represented by a thin gray line surrounding the entire cord. Dura mater and cerebrospinal fluid materials were not plotted for clarity but were included in the simulations. Color image is available online at www.liebertpub.com/neu

Maximum principal stresses in the primate models were similar to rat simulations for all levels of compression (Fig. 4). At higher compression, the primate cords showed greater peak principal strains and more contralateral cord involvement than the rat models.

In all models, the cord parenchyma shifted laterally in the canal space, thereby reducing the magnitude of impact on the cord; however, this was much more pronounced in the NHP models than the rat models for equivalent percent of dural compression. With the impactor aligned with the midline in the primate model, there was a position where the stresses and strains were maximized before there was a lateral shift, or ''popping out'' of the cord from under the impactor as the displacement increased farther (Fig. 5).

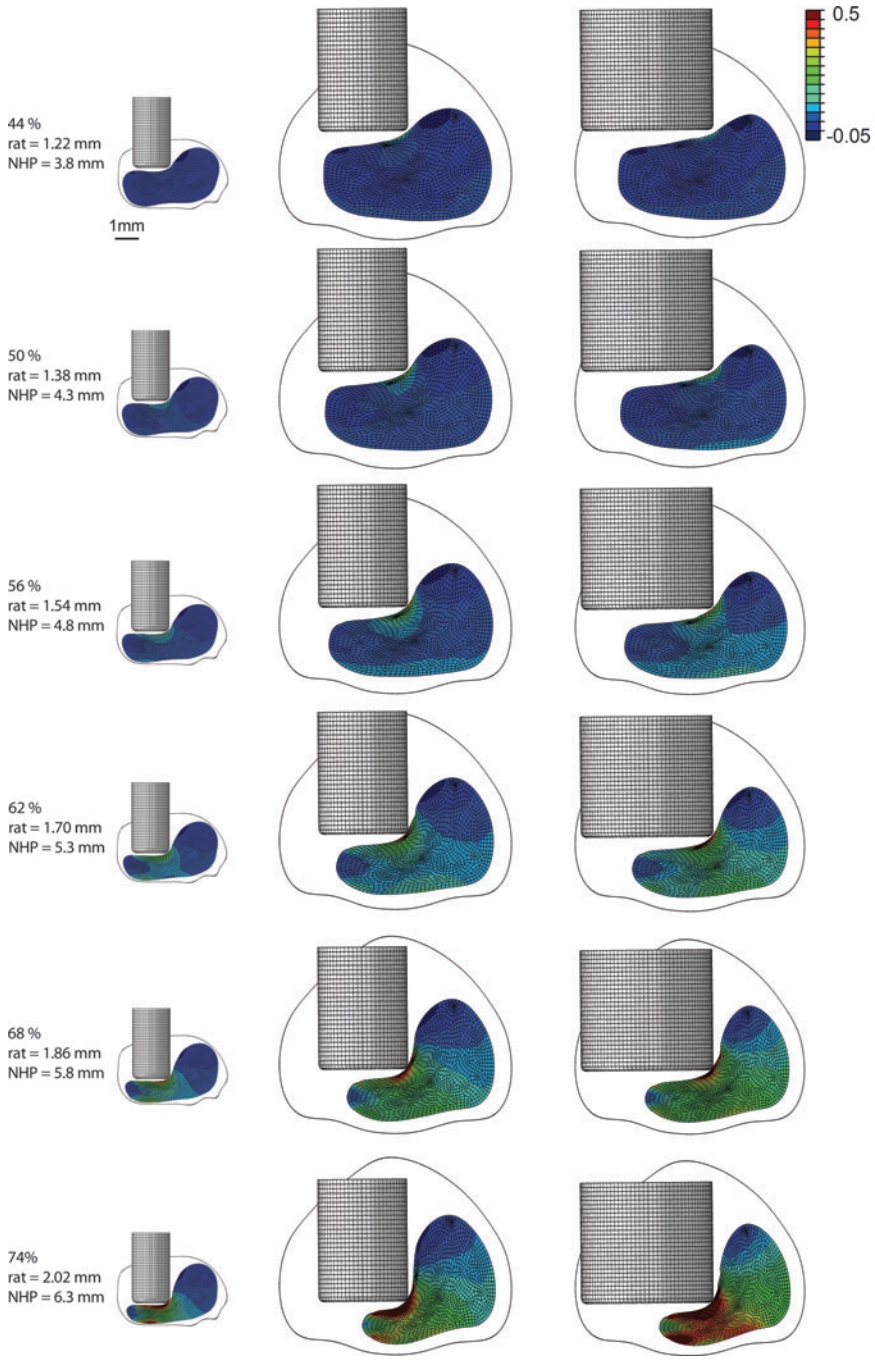

FIG. 4. Maximum principal stresses in the spinal cord resulting from unilateral contusion injuries in the rat (left) and primate (middle = 4 mm impactor, positioned 0.5 mm over midline, right = 6 mm impactor, positioned 0.5 mm over midline). Impactor peak displacement, measured from the undeformed dural surface, increases from 44% to 74% of the dural sac anterior/posterior diameter from the top to bottom rows, respectively. Stresses were similar in the rat contusion models and non-human primate (NHP) simulations for similar percent compression. Stresses concentrated at the point of contact in NHP models and only distributed below the surface under severe compression. Using a small impactor in the primate model created a more severe, focal lesion. Geometry of the vertebral canal is represented by a thin gray line surrounding the entire cord. Dura mater and cerebrospinal fluid materials were not plotted for clarity but were included in the simulations. Color image is available online at www.liebertpub.com/neu

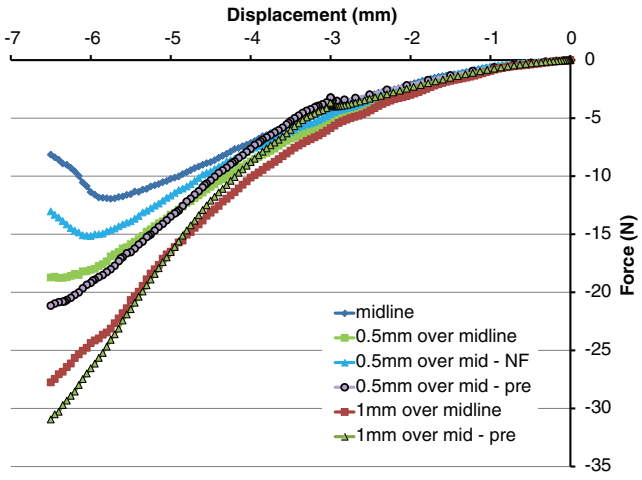

FIG. 5. Force-displacement impact mechanics for the finite element (FE) models of non-human primate unilateral contusion. Impact mechanics varied substantially with impactor alignment. Midline indicates an impact with the medial edge of the impactor aligned with the cord midline. The 0.5 mm and 1 mm are measures of the medial edge of the impactor positioned over the contralateral spinal cord. Midline impacts and impacts 0.5 mm over the midline but adjacent to the neural foramen (NF) show force reductions at peak displacement that correspond to the spinal cord popping out from under the impactor tip. Moving the impactor over the midline (mid) and pre-compressing (pre) the spinal cord resulted in less lateral shift of the cord and more tissue under the impactor to resist compression, which meant increased stiffness and peak force in the FE simulations. Color image is available online at www.liebertpub.com/neu

This lateral shift was indicated by a drop in force (Fig. 6); however, the maximum principal strains continued to increase and spread to the contralateral cord despite this lateral motion (Fig. 5).

Alignment of the impactor adjacent to the intervertebral foramen resulted in higher principal strains and greater contralateral cord involvement than impacts that were more constrained in the spinal column (Fig. 7). These higher principal strains were primarily because of tissue stretch in the rostral/caudal direction from the combination of greater displacement in the lateral direction at the injury epicenter and the restrained ends of the spinal cord.

The CSF layer in the primate model was between 2.0–2.7 mm thick; therefore, a 6.3 mm indentation from the dural surface resulted in a maximum of 3.6–4.3 mm of cord compression. The force required to generate a 6.3 mm peak displacement from the dural surface in the primate model with a 6 mm diameter impactor was seven times greater (28.6 N) than the force in the rat model (4.13 N) for a 2.02 mm impact with a 1.6 mm diameter impactor.

Given that the NHP spinal cord is approximately 8–8.5 mm in diameter along the mediolateral axis, the 6 mm impactor made first contact with the spinal cord in the central dorsal columns, thus generating a bilateral impact (Fig. 3). Reducing the size of the impactor to a 4 mm diameter impactor minimized the amount of stress and strain in the contralateral cord. Impacts with the 4 mm impactor aligned with the midline of the spinal cord, however, resulted in lateral cord motion and much lower impact forces than the 6 mm impactor (peak force = 11.95 N).

Defining a baseline for impact

Forces corresponding to surface contact with the dura and spinal cord were determined and analyzed from the surrogate cord model. Initial contact of the impactor tip with the dorsal aspect of dural surface resulted in an average force of 0.04 N. Further compression resulting in the temporary displacement of the CSF and entrapment of the spinal cord against the bottom of the vertebral canal (anterior spinal canal) resulted in a 0.47 N force (i.e., 12-fold increase in force).

Reproducibility was tested using the surrogate system, with similar results found after each trial. In addition, changes in mediolateral positioning of the impactor over the surrogate cord did not affect the resulting peak impact force. This conflicted with the FE simulations that showed stiffness responses increasing by 20% as the impactor edge moved 0.5 mm farther () over the midline during pre-load (Fig. 5). The FE simulations, however, assumed frictionless contact between the dura and spinal canal while the surrogate model did not. In the surrogate spinal cord, the 0.47 N pre-load was associated with an average of 3.1 mm of displacement from the dural surface.

Post-impact analysis and iterative model refinement

The mediolateral placement of the impactor had a significant effect on lateral motion, peak force, and patterns of stress and strain in the cord. As a result of the preliminary *in vivo* model results (subjects #1 and 2)[39] coupled with the stress and strain magnitudes observed in the NHP FE models, the medial side of the 4 mm impactor was positioned 0.5 mm and 1.0 mm over the cord center line. Moving 0.5 mm over the midline increased the peak force by 57% (18.8 N), and 1 mm over the midline increased the peak force by 132% (27.8 N) (Fig. 5).

Moving the impactor edge over the midline, however, also pushed the principal strain distribution into the contralateral spinal cord (Fig. 8). Coupling impactor alignment with pre-loading

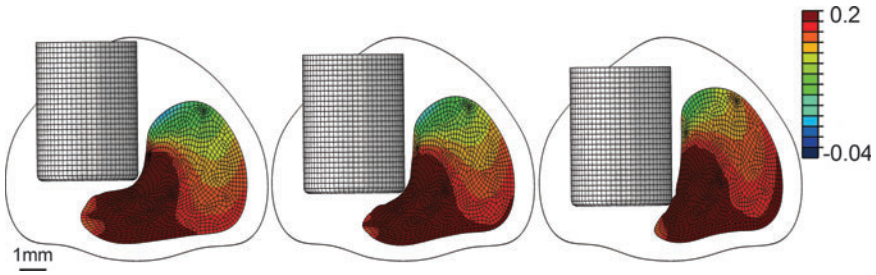

FIG. 6. Peak strains in the non-human primate model at 5.5 mm (left), 6.0 mm (middle), and 6.5 mm (right) compression measured from the undeformed dural surface when the impactor edge was aligned with the midline of the spinal cord. Between 6.0 mm and 6.5 mm compression, the cord shifts laterally and pops out from under the impactor. Although the strain patterns remain similar, peak forces were reduced 32% at 6.5 mm compression. Color image is available online at www.liebertpub.com/neu

simulations, the peak force after 3 mm of pre-load and a 3.5 mm impact with the impactor 1 mm over the midline was 31.0 N, which was 11.5% greater than a direct 6.5 mm impact without pre-load. Lateral shift of the spinal cord was also reduced by positioning the impactor 1 mm over the spinal cord midline.

Although the computational model results showed an important effect of positioning next to the intervertebral foramen in increasing lateral motion and peak principal strains, reviewing the post-injury MRIs of each *in vivo* subject showed impacts were always centered between intervertebral foramen because of the location of the laminectomy. Therefore, the intervertebral foramen did not factor into the *in vivo* experiments.

Mechanical analysis of the force-deformation response of the primate and surrogate spinal cords to impact showed non-linear behavior with a rapid drop in force between the displacement ramp and hold (Fig. 9). The force-displacement data for primate 9 showed a decrease in stiffness during the impact followed by a sharp increase. The decrease in stiffness appeared similar to the force changes seen in some of the FE simulations and likely indicated a lateral shift of the spinal cord and subsequent contact of the impactor tip with the anterolateral vertebral canal surface.

The *in vivo* spinal cord tangent stiffness characteristics were consistent across the nine study subjects (coefficient of variation was 16.5%) with the exception of Primate 5, who had a spinal cord that was half as stiff as the others. Primate 5, however, was impacted at 0.42 m/sec while the other subjects were impacted at 0.53 ± 0.03 m/sec. Similarly, the surrogate spinal cord model was highly repeatable for multiple impacts with less than 20% variation in stiffness response for varying pre-loads and peak displacements. When adjusted for pre-load, the high strain tangent stiffness of the surrogate spinal cords (3.22 N/mm) was 40% of the primate spinal cord stiffness (8.27 ± 1.36 N/mm).

Peak force in the surrogate model of impact that duplicated the experimental pre-load was less (8.5 N) than the average peak force of 16 N for the *in vivo* primate spinal cords (Table 2). The surrogate spinal cords were less stiff than the primate spinal cords, particularly at high displacements. This is likely attributed to the lack of longitudinal tension in the surrogate cord complex and lower CSF pressures than the *in vivo* system.[37]

The peak forces in the NHP FE contusion models were similar to the highest impact forces in the *in vivo* models. *In vivo* peak forces and transferred energy were highly correlated with each other.[39] Energy of the contusion impact had a peak that corresponded with peak displacement and a residual amount of energy, which was labeled ''transferred energy'' or the amount of energy absorbed by the spinal cord during the impact (Fig. 10). The energy transferred to the surrogate cord system was similar to that observed in the animal experiments with lower displacements. In addition, the proportion of energy transferred as a percent of peak energy was similar in most animal impacts and the surrogate cord model except Primates 6 and 9.

Discussion

In vivo experiments, regardless of the animal species, are often fraught with logistical and ethical challenges. The use of NHPs in experimental SCI is crucial, particularly when attempting to develop clinically relevant models that more closely replicate human mechanisms of injury. Therefore, the main aim of this study was to integrate a multidisciplinary approach to define an impact protocol combining FE and surrogate models with mechanical analyses to provide insights into the development of protocols for a unilateral, cervical contusion injury in a *Macaca mulatta,* equivalent to a previously established rat model.[19]

The mechanical measures obtained from the FE, surrogate, and *in vivo* contusion injury models provided insights into the effects of variations in alignment, pre-load, and impact severity on expected injury outcomes. FE[34,35] and surrogate[37] models were constructed from MRIs of the *Macaca mulatta* cervical vertebral spine and spinal cord parenchyma using established methods. To our knowledge, this is the first study to detail the use of such FE and surrogate models to establish impact parameters to define a new primate SCI model, before and in parallel with *in vivo* experiments.

Overall, both the FE and surrogate models showed good agreement with the *in vivo* experimental impact mechanics (displacement, force, velocity, and energy). The force-displacement characteristics of the FE and surrogate cord models demonstrated consistent findings to those observed in the NHP *in vivo* study.[39] The FE model was better able to replicate the impact behavior of the spinal cord and provided the opportunity to visualize stress and strain distributions in the tissue as well as bulk tissue motion resulting from the acute impact.

We know that differences in gray and white matter properties, however, affect the distributions of stresses and strains in the compressed spinal cord,[48] but there are currently insufficient experimental data to accurately differentiate these material characteristics in an *in vivo* model. In contrast, the surrogate cord model provided critical input into the low rate pre-loading to displace the CSF from around the spinal cord.

It is noteworthy that both of these models were limited to data analysis from isolated segments of the spinal cord when compared with the intact *in vivo* spinal cord. These results, however, demonstrated good mechanical fidelity with the *in vivo* impact suggesting that modeling of isolated cord segments did not have a significant effect on impact mechanics. This is in agreement with other studies investigating the effect of model length on injury mechanics, where minimal changes in outcomes were detected because of the localized nature of contusion impacts.[35]

With increased CSF space of the NHP contusion impact, however, the length of the modeled cord segment may affect rostral/caudal (longitudinal) tension in the model because the positions of the ends of the cord were fixed. A study of human surrogate SCI mechanics showed longitudinal tensile forces restraining the ends of the spinal cord increased four-fold with increased CSF thickness.[37] Using MRI to construct the FE and surrogate cord models improved the geometric fidelity of the models over generic representations of the tissue; however, the models did not simulate the geometric variability seen in animal subjects. For example, in a controlled population of *Macaca mulatta,* the cord dimensions varied by ±10%,[40] which could affect the peak force results. This potential source of variation led to the introduction of pre-impact MRIs as part of the *in vivo* injury protocol.[39]

FIG. 7. Peak strains in the non-human primate models with the cord adjacent to the vertebral column (left) or intervertebral foramen (right) for 6.5 mm compression measured from the undeformed dural surface when the impact edge was aligned with the midline of the spinal cord. Peak strains were greater next to the intervertebral foramen primarily because of increased longitudinal strains from the lateral motion of the cord. Color image is available online at www.liebertpub.com/neu

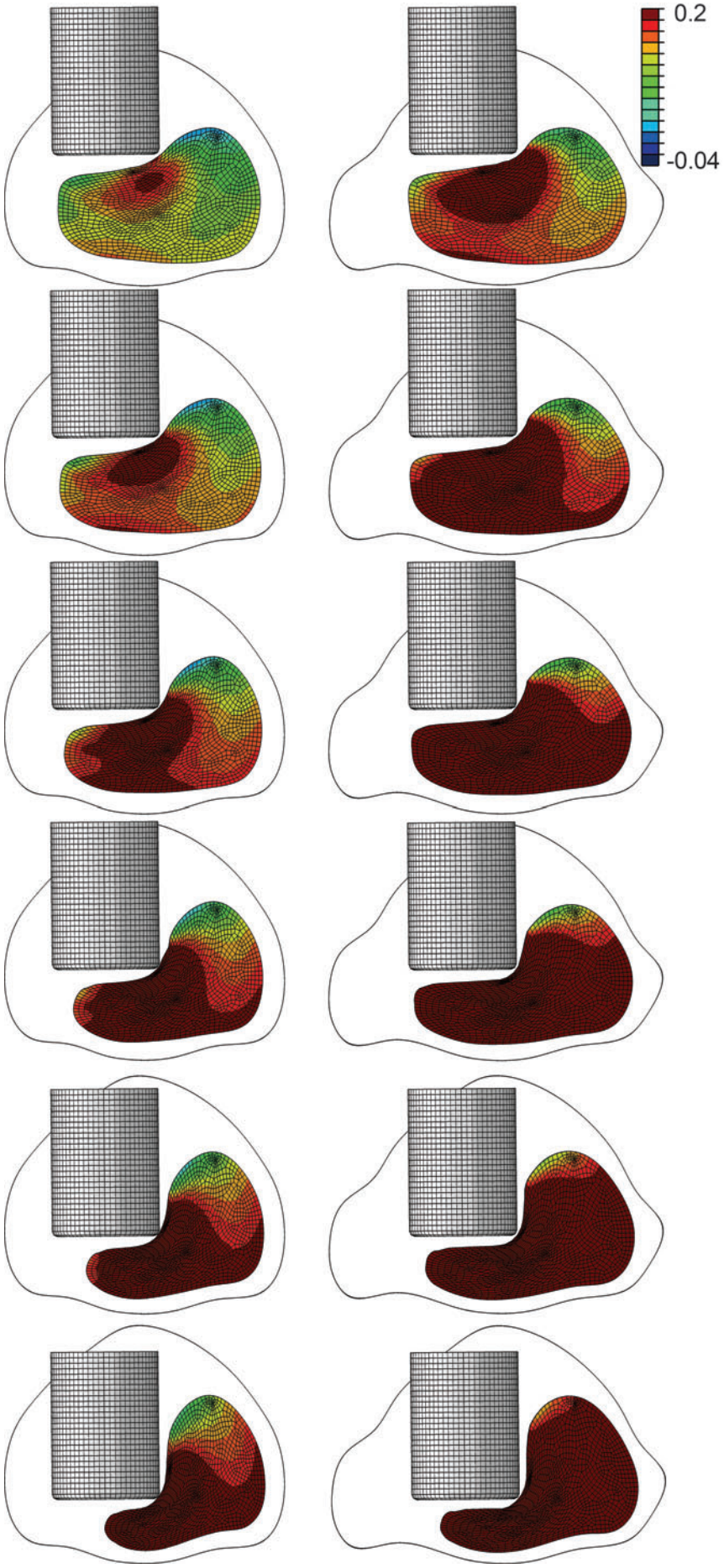
0.2
-0.04

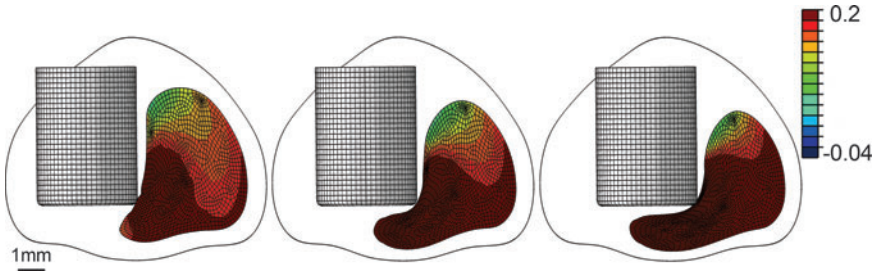

FIG. 8. Peak strains in the non-human primate model with the medial impactor tip edge positioned at 0 mm (left), –0.5 mm (middle), and –1.0 mm (right) relative to the midline. Negative measures indicate the impactor edge was over the midline on the contralateral side. Peak displacement from the undeformed dural surface was 6.5 mm for all impacts. Peak strain distributions show a strong effect of impactor alignment will little tissue under the impactor when the tip was aligned with the midline of the cord. Moving the impactor tip over the midline increased the spread of strains in the spinal cord to the contralateral side. Color image is available online at www.liebertpub.com/neu

The results predicted by the FE and surrogate models effectively bounded the *in vivo* model results and may reflect the differences in the end constraints for each model. The surrogate model had no end constraints while the FE model had fully fixed cord ends. The *in vivo* spinal cord falls somewhere between these extremes. The rat FE model of unilateral injury predicted a peak force of 2.53 N for 1.6 mm injuries at a rate of 120 mm/sec with a 1.6 mm diameter impactor. This compares with peak forces of 2.0 N[30] observed in models using a 1.6 mm diameter impactor to a depth of 1.6 mm and a rate of 120 mm/sec.

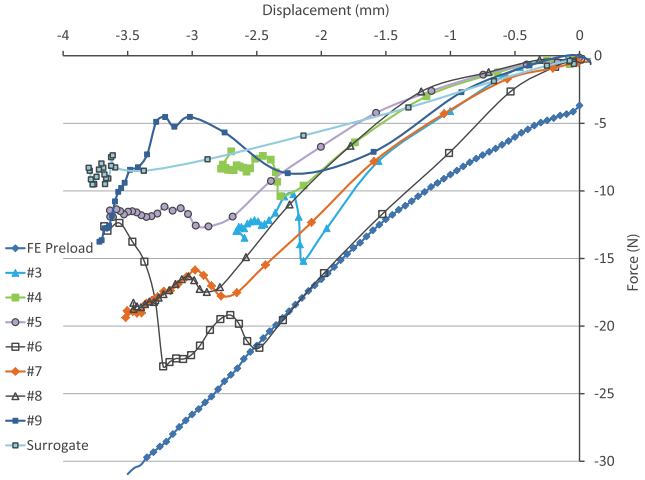

FIG. 9. Force-displacement impact mechanics for *in vivo* non-human primate contusion injuries compared with the finite element (FE) simulation and surrogate spinal cord model mechanics. The *in vivo* spinal cord stiffness (slope of the force-deformation curve) was similar for all animals independent of variations in the peak displacement and peak force applied to the spinal cord (Table 2). Peak displacement was measured starting from zero as the final pre-load position. Subjects 3 and 4 had a peak displacement of 2.72 mm while subjects 6 through 9 had a peak displacement of 3.60 mm. Subject 5 had a peak displacement of 3.64 mm but a slower impact velocity (0.42 m/sec) than the other subjects (average 0.53 m/sec). The surrogate and FE models were less stiff than the *in vivo* tissues. There is a shift in the peak force for each impact because of a change in compression velocity from the ramp to dwell phase. The impactor system was being driven at its maximum velocity (0.55 m/sec) to achieve these impacts; therefore, peak displacement did not occur in most impacts until the end of the dwell signal phase. Primate 9 shows a distinctive and rounded peak after 5 mm of total compression (2 mm of dynamic impact), which is indicative of the cord slipping out from under the impactor. Therefore, the peak force recorded for Primate 9 reflects contact with the spinal canal and not force applied directly to the spinal cord. Color image is available online at www.liebertpub.com/neu

Weight drop models using a 2 mm impactor had energies ranging from 0.61 to 2.45 millijoules (mJ) for moderate severity injuries.[19,41,49] The peak energy in the rat FE model was 1.41 mJ for a 1.6 mm impactor to an impact depth of 2.02mm. A weight drop model of NHP bilateral thoracic contusion used a 500g-cm (50 mJ) impact and a 6 mm diameter impactor to generate a moderate injury in the spinal cord.[30] This compares with an averaged peak energy of 244 ± 110g-cm (24.4 ± 11.0 mJ) and a maximum peak energy of 439g-cm (43.9 mJ) observed in primate 6, one of the most injured test subjects.

The surrogate model results were within the lower range of stiffness responses observed in the primate injury models. This may be explained by the lack of tethering of the surrogate cord ends within the canal space. For simplicity and ease of use, the surrogate cord model was sealed in fluid filled polyethylene tubing but was not constrained on either end. A surrogate model of a human spinal cord showed increased tethering forces (up to 3 N) during impact for increasing CSF thickness at moderate severity impact, which was attributed to the amount of travel before the cord contacted the opposing canal surface.[37] As a result, the untethered spinal cord will underestimate the forces at high displacements. These results suggest that introducing traction in the *in vivo* model, similar to protocols used in rat contusion,[50] may help to standardize the impact mechanics.

The FE simulations of the primate injury highlighted a significant problem of lateral shift of the spinal cord during unilateral contusion, which has been discussed in previous rodent unilateral contusion models.[25] In addition, the NHP FE models highlighted a lateral shift of the cord that occurs at high levels of compression. Therefore, simply increasing the magnitude of compression in the NHP *in vivo* model is unlikely to increase the severity of the inflicted injury.

To counteract the lateral shift, one solution in the rat model was to angle the direction of the impactor by 22.5 degrees to eliminate the effect of bulk cord motion.[28] In the primate, rotating the subject under the impactor is not feasible because of its size and weight. Similarly, rotating the impactor and actuator would require much larger structural fixtures to stabilize the actuator, which would impede surgical access and would require a significant increase in the size of the surgical exposure because of the depth of the spinal canal within the primate (4–5 cm).

Pre-loading the spinal cord to effectively trap the cord under the impactor and positioning the impactor over the midline were shown

Table 2. Biomechanical Impact Parameters and Outcomes for each *in vivo* Impact, Surrogate Model, and Finite Element Simulation

	Subject #3	*Subject #4*	*Subject #5*	*Subject #6*	*Subject #7*	*Subject #8*	*Subject #9*	*Surrogate*	*FE model*
Pre-load									
Depth from dural surface (mm)	2.5	3.0	3.6	3.0	3.2	3.5	2.8	2.5	3.0
Pre-load force (N)	–0.30	–0.30	–0.40	–0.56	–0.33	–0.28	–0.18	–0.50	–3.23
ML position (mm)	–1.0	–1.0	–1.0	–1.0	–1.0	–0.5	0.0	0.0	–0.5
Impact									
Velocity (m/s)	0.55	0.55	0.42	0.48	0.51	0.51	0.58	0.55	0.50
Displacement (mm)	–2.66	–2.78	–3.64	–3.68	–3.52	–3.46	–3.72	–3.65	–3.50
Peak force (N)	–14.90	–10.54	–12.50	–23.19	–19.15	–18.73	–13.40	–8.5	–21.2
Peak energy (mJ)	17.77	12.92	22.67	46.16	33.93	27.44	19.89	19.17	n/a
Transferred energy (mJ)	8.86	7.91	12.86	37.93	20.11	16.21	16.48	10.86	n/a

FE, finite element; ML, mediolateral.

in FE simulations to reduce the degree of lateral shift during the impact and engage a significant portion of the ipsilateral spinal cord. The usefulness of this strategy was confirmed in the *in vivo* study. Eliminating the impact dissipating effect of the CSF layer through pre-compression constrained the injury to the ipsilateral spinal cord.

Unlike other contusion injury models, the intent of the unilateral impact is to create an injury that is limited to the ipsilateral spinal cord to avoid bilateral motor deficit. In the rat model, the thin CSF layer does not significantly affect the spread of the impact; however, in the primate, with a thicker dura and CSF layer, the fluid acts to distribute the impact load across and along the spinal cord.[36] This protective mechanism minimizes high strains in the tissue to reduce the severity of injury; however, for these models, the CSF layer distributes the effect of the impact to the contralateral side, thereby defeating the purpose of developing a unilateral injury model. Removing the protective effect of the CSF from this primate contusion injury model may affect the biomechanical fidelity of this injury model when compared with humans but is critical for creating a focal, unilateral impact.

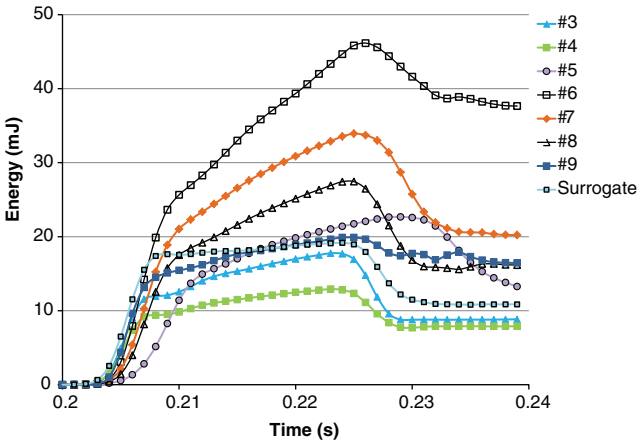

FIG. 10. Energy corresponding to each contusion impact. The energy was greatest at peak displacement and was reduced as the impactor retracted from the spinal cord surface. The residual energy after impactor retraction was the transferred energy. Subjects 3 and 4 had an average peak impact of 2.72 mm while subjects 6 through 9 had average peak impacts of 3.60 mm. Subject 5 shows a different initial energy/time ramp because of the slower impact velocity (0.42 m/sec vs. an average 0.53 m/sec) than the other tests. The energy curve for Primate 9 shows no decrease in energy after impactor retraction providing further evidence of an abnormal impact. The energy curve for the surrogate cord is similar to non-human primate impacts with lower displacement. Color image is available online at www.liebertpub.com/neu

Although maximum principal strains have been proposed as the measure that best correlates with injury in small animal models[35] and *in vitro*[51] tests on isolated axons, tissue stresses are more likely to correlate with ischemic injury.[52,53] Therefore, studying both outcomes in FE models is important for fully characterizing the relationship between tissue mechanics and damage. Results from the FE analysis showed similar levels of maximum principal stresses for equivalent magnitudes of a/p dural sac compression in the rat and NHP models. At maximum compression, however, the stresses increased in the NHP model as the cord moved laterally in the canal space and was pinched against the lateral spinal canal.

Maximum principal strains were similar in the rat and NHP FE models for compression below 50%. At higher levels of compression, the NHP models showed greater strain distribution to the anterior and contralateral spinal cord. When compared with *in vivo* outcomes, impacts of 58–67% compression (1.6–1.8 mm) resulted in moderate severity injuries in the rat,[29] while impacts of 58% (3 mm pre-load and 2 mm impact) resulted in no measurable functional or histological damage in the NHP model.[39] Impacts of 67–85% (5.74–7.24 mm) were required to generate residual deficits in the NHP model.[39] Therefore, the FE models presented in this study provided overall trends in injury severity predictions and highlighted the relative effects of lateral cord shift but could not directly predict the severity of tissue damage.

In carefully controlled small animal studies and tissue cultures, the study population is homogeneous in many ways, with weight, age, anesthesia dosage, and surgical timing standardized.[27] Peak impact depth correlates closely with peak impact forces and energy in those models.[16,23,25] That level of parameter control is not feasible in NHP models of injury, however, and there was not a strong correlation between peak displacement and peak force (Pearson correlation = 0.525).[39] The variations in peak impact force and energy that correspond to a consistent impact distance suggest that NHP injury severity cannot be characterized by a single mechanical measure of injury and that injury mechanics (displacement, force, velocity, and energy) should be fully described for comparison across studies.

The pre-load forces identified using the surrogate cord model may have led to a greater degree of pre-compression in the *in vivo* spinal cords, because the surrogate cord properties do not show the same viscoelastic characteristics as the *in vivo* spinal cord.[38] The *in vivo* spinal cord is less stiff than the surrogate cord at low loading rates such as those used to apply the pre-load. In addition, the pre-load was applied by manually advancing the impactor tip because force control of the injury system at these loads can lead to instability.

Variations in the rate of pre-load application and pauses to confirm load readings and position allow tissue relaxation and affect the force reading. Using a sinusoidal pre-load protocol could remove an element of the rate effect by ensuring the cord is loaded at a cyclic 50 Hz signal.[25] In addition, knowing that the *in vivo* cord stiffness was similar for all animals in the study, tracking the relationship between force and depth of compression during the pre-load protocol should further standardize the definition of the baseline for impact. Successful *in vivo* impacts with proper alignment had a minimum pre-load force of 0.3 N for a displacement of 3.0 mm.

The mechanics of the unilateral impact and the tissue level stresses and strains were greatly affected by small changes (0.5 mm) in impactor alignment unlike central contusion models, which show very little effect of impactor alignment on impact mechanics.[34] Positioning the impactor tip over the midline (0.5 mm or 1 mm) reduced the lateral shift effects in the FE simulations and did not result in contralateral injuries in the *in vivo* models.[39] Improving our ability to landmark the spinal cord midline will be critical in reducing the variability in impact mechanics and injury outcomes.

The FE simulations and the *in vivo* injury model results showed lateral white matter sparing except in the most severe impacts. Interestingly, the FE simulations showed less lateral white matter sparing as the impactor was moved over the contralateral midline. White matter sparing at the injury site is well correlated with functional recovery[54–56] and may be an important source of *in vivo* model variability. Pre-impact imaging and subject-specific models can assist in defining the appropriate impact parameters, degree of pre-load, and landmarks for impactor alignment to reduce outcome variability and improve the sensitivity of these models for detecting treatment effects. Reduced injury variation would reduce the number of animals required for statistical significance.

Post-impact mechanical analyses can highlight potential sources of error or variability in the *in vivo* injury models. Primate 9 showed an unpredicted change in force during contusion (Fig. 9). At that time, we suspected that the cord had shifted laterally and the impactor had contacted the vertebral canal during impact. Our interpretations were confirmed during necropsy when an abnormal curvature in the cervical spinal column was discovered. Primate 6 had the highest peak impact forces but showed a sudden drop in force before peak displacement, which may reflect movement in the vertebral clamps under high load.

Column morphology can also be affected by the laminectomy performed to expose the spinal cord for impact, and injury mechanics can be affected by the laminectomy size.[25] The FE models of the spinal cord showed rotation of the cord in the canal space as the impactor advanced. Lateral motion and rotation of the cord was limited by the ventral spinal canal boundary.

If the laminectomy removes bone from the contralateral side, this constraining effect will be reduced. This was observed in primate 8 who had a laminectomy measuring 12 mm wide, which was 4 mm wider than the average laminectomy. Despite similar force and displacement parameters, Primate 8 had significantly less functional deficits and less tissue damage than Primate 7. Consistent injury outcomes depend on an accurate and consistent laminectomy size and location.[39]

This mechanical analysis of primate contusion injury demonstrated the importance of cord and column morphology on impact. Lateral shift of the spinal cord during impact was much greater than that observed in smaller animal models of contusion injury. Slowly pre-compressing the spinal cord to displace the CSF before impact and positioning the edge of the impactor tip 0.5–1.0 mm over the cord midline resulted in a moderate severity injury, isolated mostly in the ipsilateral spinal cord.

Despite careful control of the impact parameters (pre-load, displacement, and velocity), however, there was variation in the functional and histological outcomes of the *in vivo* NHP contusion injury model.[39] Importantly, dependent variables of peak force, peak energy, and transferred energy correlated with functional outcomes, which highlight the need to report the controlled pre-load and injury parameters as well as the observed resulting injury mechanics to fully characterize a contusion impact in the NHP.

In smaller animal models, large numbers of animals are used to establish consistent impact parameters to define a standardized injury model. When primates are used, it is ethically and economically essential to minimize the number of live animals needed for a study. The combination of FE models, surrogate models, and *in vivo* studies has highlighted the need to define and report multiple mechanical parameters—impact depth, velocity, force, and energy to fully characterize the contusion injury. In addition, accurately defining the injury baseline (pre-load force and alignment) is critical for developing a consistent injury protocol.

Mechanical analyses provided important insights into the sources of variability in a large animal contusion model. An NHP model of SCI with persistent, moderate-severity deficits will be useful for evaluating therapeutic interventions in a clinically relevant model of SCI.

Acknowledgments

This work was supported by grants from the Natural Sciences and Engineering Research Council of Canada (EQPE-Q407572, RGPIN-402007), the NIH (R-01 NS042291), the VA, and the CH Neilsen Foundation.

Author Disclosure Statement

No competing financial interests exist.

References

1. Wagner, F.C., Jr, and Chehrazi, B. (1982). Early decompression and neurological outcome in acute cervical spinal cord injuries. J. Neurosurg. 56, 699–705.
2. Tator, C.H. (1983). Spine-spinal cord relationships in spinal cord trauma. Clin. Neurosurg. 30, 479–494.
3. Allen, A.R. (1911). Surgery of experimental lesion of spinal cord equivalent to crush injury of fracture dislocation of spinal column: a preliminary report. J Am Med Assoc 57, 878–880.
4. Kwon, B.K., Oxland, T.R., and Tetzlaff, W. (2002). Animal models used in spinal cord regeneration research. Spine (Phila Pa 1976) 27, 1504–1510.
5. Clarke, E.C., and Bilston, L.E. (2008). Contrasting biomechanics and neuropathology of spinal cord injury in neonatal and adult rats following vertebral dislocation. J. Neurotrauma 25, 817–832.

6. Clarke, E C., Choo, A.M., Liu, J., Lam, C.K., Bilston, L.E., Tetzlaff, W., and Oxland, T.R. (2008). Anterior fracture-dislocation is more severe than lateral: a biomechanical and neuropathological comparison in rat thoracolumbar spine. J. Neurotrauma 25, 371–383.
7. Choo, A.M., Liu, J., Liu, Z., Dvorak, M., Tetzlaff, W., and Oxland, T.R. (2009). Modeling spinal cord contusion, dislocation, and distraction: characterization of vertebral clamps, injury severities, and node of Ranvier deformations. J. Neurosci. Methods 181, 6–17.
8. Choo, A.M., Liu, J., Dvorak, M., Tetzlaff, W., and Oxland, T.R. (2008). Secondary pathology following contusion, dislocation, and distraction spinal cord injuries. Exp. Neurol. 212, 490–506.
9. Tator, C.H. (2006). Review of treatment trials in human spinal cord injury: issues, difficulties, and recommendations. Neurosurgery 59, 957–987.
10. Courtine, G., Bunge, M.B., Fawcett, J.W., Grossman, R.G., Kaas, J.H., Lemon, R., Maier, I., Martin, J., Nudo, R.J., Ramon-Cueto, A., Rouiller, E.M., Schnell, L., Wannier, T., Schwab, M.E., and Edgerton, V.R. (2007). Can experiments in nonhuman primates expedite the translation of treatments for spinal cord injury in humans? Nat. Med. 13, 561–566.
11. Sledge, J., Graham, W.A., Westmoreland, S., Sejdic, E., Miller, A., Hoggatt, A., and Nesathurai, S. (2013). Spinal cord injury models in non human primates: Are lesions created by sharp instruments relevant to human injuries? Med. Hypotheses 81, 747–748.
12. Rosenzweig, E.S., Courtine, G., Jindrich, D.L., Brock, J.H., Ferguson, A.R., Strand, S.C., Nout, Y.S., Roy, R.R., Miller, D.M., Beattie, M.S., Havton, L.A., Bresnahan, J.C., Edgerton, V.R., and Tuszynski, M.H. (2010). Extensive spontaneous plasticity of corticospinal projections after primate spinal cord injury. Nat. Neurosci. 13, 1505–1510.
13. Kwon, B.K., Streijger, F., Hill, C.E., Anderson, A.J., Bacon, M., Beattie, M.S., Blesch, A., Bradbury, E.J., Brown, A., Bresnahan, J.C., Case, C.C., Colburn, R.W., David, S., Fawcett, J.W., Ferguson, A.R., Fischer, I., Floyd, C.L., Gensel, J.C., Houle, J.D., Jakeman, L.B., Jeffery, N.D., Jones, L.A., Kleitman, N., Kocsis, J., Lu, P., Magnuson, D.S., Marsala, M., Moore, S.W., Mothe, A.J., Oudega, M., Plant, G.W., Rabchevsky, A.S., Schwab, J.M., Silver, J., Steward, O., Xu, X.M., Guest, J.D., and Tetzlaff, W. (2015). Large animal and primate models of spinal cord injury for the testing of novel therapies. Exp. Neurol. 269, 154–168.
14. Friedli, L., Rosenzweig, E.S., Barraud, Q., Schubert, M., Dominici, N., Awai, L., Nielson, J.L., Musienko, P., Nout-Lomas, Y., Zhong, H., Zdunowski, S., Roy, R.R., Strand, S.C., van den Brand, R., Havton, L.A., Beattie, M.S., Bresnahan, J.C., Bezard, E., Bloch, J., Edgerton, V.R., Ferguson, A.R., Curt, A., Tuszynski, M.H., and Courtine, G. (2015). Pronounced species divergence in corticospinal tract reorganization and functional recovery after lateralized spinal cord injury favors primates. Sci. Transl. Med. 7, 302ra134.
15. Basso, D.M. (2000). Neuroanatomical substrates of functional recovery after experimental spinal cord injury: implications of basic science research for human spinal cord injury. Phys. Ther. 80, 808–817.
16. Behrmann, D.L., Bresnahan, J.C., Beattie, M.S., and Shah, B.R. (1992). Spinal cord injury produced by consistent mechanical displacement of the cord in rats: behavioral and histologic analysis. J. Neurotrauma 9, 197–217.
17. Bresnahan, J.C., Beattie, M. S., Todd, F.D., 3rd, and Noyes, D.H. (1987). A behavioral and anatomical analysis of spinal cord injury produced by a feedback-controlled impaction device. Exp. Neurol. 95, 548–570.
18. Dunham, K A., Siriphorn, A., Chompoopong, S., and Floyd, C.L. (2010). Characterization of a graded cervical hemicontusion spinal cord injury model in adult male rats. J. Neurotrauma 27, 2091–2106.
19. Gensel, J.C., Tovar, C.A., Hamers, F.P., Deibert, R.J., Beattie, M.S., and Bresnahan, J.C. (2006). Behavioral and histological characterization of unilateral cervical spinal cord contusion injury in rats. J. Neurotrauma 23, 36–54.
20. Ma, M., Basso, D.M., Walters, P., Stokes, B.T., and Jakeman, L.B. (2001). Behavioral and histological outcomes following graded spinal cord contusion injury in the C57Bl/6 mouse. Exp. Neurol. 169, 239–254.
21. Nishi, R.A., Liu, H., Chu, Y., Hamamura, M., Su, M.Y., Nalcioglu, O., and Anderson, A.J. (2007). Behavioral, histological, and ex vivo magnetic resonance imaging assessment of graded contusion spinal cord injury in mice. J. Neurotrauma 24, 674–689.
22. Streijger, F., Beernink, T.M., Lee, J.H., Bhatnagar, T., Park, S., Kwon, B.K., and Tetzlaff, W. (2013). Characterization of a cervical spinal cord hemicontusion injury in mice using the infinite horizon impactor. J. Neurotrauma 30, 869–883.
23. Sparrey, C.J., Choo, A.M., Liu, J., Tetzlaff, W., and Oxland, T.R. (2008). The distribution of tissue damage in the spinal cord is influenced by the contusion velocity. Spine (Phila Pa 1976) 33, E812–819.
24. Scheff, S.W., Rabchevsky, A.G., Fugaccia, I., Main, J.A., and Lumpp Jr, J.E. (2003). Experimental modeling of spinal cord injury: characterization of a force-defined injury device. J. Neurotrauma 20, 179–193.
25. Stokes, B.T., Noyes, D.H., and Behrmann, D.L. (1992). An electromechanical spinal injury technique with dynamic sensitivity. J. Neurotrauma 9, 187–195.
26. Kwo, S., Young, W., and Descrescito, V. (1989). Spinal cord sodium, potassium, calcium, and water concentration changes in rats after graded contusion injury. J. Neurotrauma 6, 13–24.
27. Young, W. (2002). Spinal cord contusion models. Prog. Brain Res. 137, 231–255.
26. Lee, J.H., Streijger, F., Tigchelaar, S., Maloon, M., Liu, J., Tetzlaff, W., and Kwon, B.K. (2012). A contusive model of unilateral cervical spinal cord injury using the infinite horizon impactor. J. Vis. Exp. (65). pii: 3313.
29. Sandrow, H.R., Shumsky, J.S., Amin, A., and Houle, J.D. (2008). Aspiration of a cervical spinal contusion injury in preparation for delayed peripheral nerve grafting does not impair forelimb behavior or axon regeneration. Exp. Neurol. 210, 489–500.
30. Bresnahan, J.C., King, J.S., Martin, G.F., and Yashon, D. (1976). A neuroanatomical analysis of spinal cord injury in the rhesus monkey (Macaca mulatta). J. Neurol. Sci. 28, 521–542.
31. Iwanami, A., Yamane, J., Katoh, H., Nakamura, M., Momoshima, S., Ishii, H., Tanioka, Y., Tamaoki, N., Nomura, T., Toyama, Y., and Okano, H. (2005). Establishment of graded spinal cord injury model in a nonhuman primate: the common marmoset. J. Neurosci. Res. 80, 172–181.
32. Ouyang, H., Galle, B., Li, J., Nauman, E., and Shi, R. (2008). Biomechanics of spinal cord injury: a multimodal investigation using ex vivo guinea pig spinal cord white matter. J. Neurotrauma 25, 19–29.
33. Galle, B., Ouyang, H., Shi, R., and Nauman, E. (2007). Correlations between tissue-level stresses and strains and cellular damage within the guinea pig spinal cord white matter. J. Biomech. 40, 3029–3033.
34. Maikos, J.T., Qian, Z., Metaxas, D., and Shreiber, D.I. (2008). Finite element analysis of spinal cord injury in the rat. J. Neurotrauma 25, 795–816.
35. Russell, C.M., Choo, A.M., Tetzlaff, W., Chung, T.E., and Oxland, T.R. (2012). Maximum principal strain correlates with spinal cord tissue damage in contusion and dislocation injuries in the rat cervical spine. J. Neurotrauma 29, 1574–1585.
36. Persson, C., Summers, J., and Hall, R.M. (2011). The importance of fluid-structure interaction in spinal trauma models. J. Neurotrauma 28, 113–125.
37. Jones, C.F., Kwon, B.K., and Cripton, P.A. (2012). Mechanical indicators of injury severity are decreased with increased thecal sac dimension in a bench-top model of contusion type spinal cord injury. J. Biomech. 45, 1003–1010.
38. Kroeker, S.G., Morley, P.L., Jones, C.F., Bilston, L E., and Cripton, P.A. (2009). The development of an improved physical surrogate model of the human spinal cord—tension and transverse compression. J. Biomech. 42, 878–883.
39. Salegio, E.A., Bresnahan, J.C., Sparrey, C.J., Camisa, W., Fischer, J., Leasure, J., Buckley, J., Nout-Lomas, Y., Rosenzweig, E., Moseanko, R., Strand, S.C., Hawbecker, S., Lemoy, M., Ma, X., Haefeli, J., Nielson, J.L., Edgerton, V.R., Ferguson, A.R., Tuszynski, M.H., and Beattie, M.S. (2015). A unilateral cervical spinal cord contusion injury model in nonhuman primates (Macaca mulatta). J. Neurotrauma. Epub ahead of print. DOI 10.1089/neu.2015–3956.
40. Romanowski, K., Nout, Y.S., Beattie, M.S., Bresnahan, J.C., and Sparrey, C.J. (2011). Interspecies variation in spinal cord and column morphology and its affect on cord compression mechanics. Society for Neuroscience, Washington, DC.
41. Mihai, G., Nout, Y.S., Tovar, C.A., Miller, B.A., Schmalbrock, P., Bresnahan, J.C., and Beattie, M.S. (2008). Longitudinal comparison of two severities of unilateral cervical spinal cord injury using magnetic resonance imaging in rats. J. Neurotrauma 25, 1–18.
42. Hong, J.Y., Suh, S.W., Park, S.Y., Modi, H.N., Rhyu, I.J., Kwon, S., Yu, H., and Byun, J. (2011). Analysis of dural sac thickness in human

spine-cadaver study with confocal infrared laser microscope. Spine J. 11, 1121–1127.
43. Zarzur, E. (1996). Mechanical properties of the human lumbar dura mater. Arq Neuropsiquiatr 54, 455–460.
44. Persson, C., Evans, S., Marsh, R., Summers, J.L., and Hall, R.M. (2010). Poisson's ratio and strain rate dependency of the constitutive behavior of spinal dura mater. Ann. Biomed. Eng. 38, 975–983.
45. Maikos, J.T., Elias, R.A., and Shreiber, D.I. (2008). Mechanical properties of dura mater from the rat brain and spinal cord. J. Neurotrauma 25, 38–51.
46. Clarke, E.C. (2011). Spinal cord mechanical properties, in: *Neural Tissue Biomechanics*. Springer: New York, pps. 25–40.
47. Chafi, M.S., Dirisala, V., Karami, G., and Ziejewski, M. (2009). A finite element method parametric study of the dynamic response of the human brain with different cerebrospinal fluid constitutive properties. Proc. Inst. Mech. Eng. H. 223, 1003–1019.
48. Sparrey, C.J., Manley, G.T., and Keaveny, T.M. (2009). Effects of white, grey, and pia mater properties on tissue level stresses and strains in the compressed spinal cord. J. Neurotrauma 26, 585–595.
49. Soblosky, J.S., Song, J., and Dinh, D.H. (2001). Graded unilateral cervical spinal cord injury in the rat: evaluation of forelimb recovery and histological effects. Behav. Brain. Res. 119, 1–13.
50. Sparrey, C.J. (2004). The effect of impact velocity on acute spinal cord injury. Master's thesis, University of British Columbia.
51. Galbraith, J.A., Thibault, L.E., and Matteson, D.R. (1993). Mechanical and electrical responses of the squid giant axon to simple elongation. J. Biomech. Eng. 115, 13–22.
52. Carlson, G.D., Minato, Y., Okada, A., Gorden, C.D., Warden, K.E., Barbeau, J.M., Biro, C.L., Bahnuik, E., Bohlman, H H., and Lamanna, J.C. (1997). Early time-dependent decompression for spinal cord injury: vascular mechanisms of recovery. J. Neurotrauma 14, 951–962.
53. Carlson, G.D., Gorden, C.D., Nakazowa, S., Wada, E., Warden, K., and LaManna, J.C. (2000). Perfusion-limited recovery of evoked potential function after spinal cord injury. Spine (Phila Pa 1976) 25, 1218–1226.
54. Lee, J.H., Jones, C.F., Okon, E.B., Anderson, L., Tigchelaar, S., Kooner, P., Godbey, T., Chua, B., Gray, G., Hildebrandt, R., Cripton, P., Tetzlaff, W., and Kwon, B.K. (2013). A novel porcine model of traumatic thoracic spinal cord injury. J. Neurotrauma 30, 142–159.
55. Tu, T.W., Kim, J.H., Yin, F.Q., Jakeman, L.B., and Song, S.K. (2013). The impact of myelination on axon sparing and locomotor function recovery in spinal cord injury assessed using diffusion tensor imaging. NMR Biomed. 26, 1484–1495.
56. Kelley, B. J., Harel, N. Y., Kim, C. Y., Papademetris, X., Coman, D., Wang, X., Hasan, O., Kaufman, A., Globinsky, R., Staib, L. H., Cafferty, W. B., Hyder, F., and Strittmatter, S. M. (2014). Diffusion tensor imaging as a predictor of locomotor function after experimental spinal cord injury and recovery. J. Neurotrauma 31, 1362–1373.

Address correspondence to:
Carolyn J. Sparrey, PhD
Simon Fraser University
250-13450 102 Avenue
Surrey, British Columbia V3T 0A3
Canada

E-mail: csparrey@sfu.ca